Generation of a single attosecond pulse from an overdense plasma surface driven by a laser pulse with time-dependent polarization*

Luo Mu-Hua(罗牧华) and Zhang Qiu-Ju(张秋菊)†

College of Physics and Electronics, Shandong Normal University, Jinan 250014, *China*

(Received 24 December 2010; revised manuscript received 1 April 2011)

The influence of time-dependent polarization on attosecond pulse generation from an overdense plasma surface driven by laser pulse is discussed analytically and numerically. The results show that the frequency of controlling pulse controls the number and interval of the generated attosecond pulse, that the generation moment of the attosecond pulse is dominated by the phase difference between the controlling and driving pulses, and that the amplitude of the controlling pulse affects the intensity of the attosecond pulse. Using the method of time-dependent polarization, a "single" ultra-strong attosecond pulse with duration $\tau \approx 8.6$ as and intensity $I \approx 3.08 \times 10^{20}$ W·cm^{-2} can be generated.

Keywords: attosecond pulse, overdense plasma, particle-in-cell simulation

PACS: 52.38.Ph, 52.59.Hq, 52.65.Rr **DOI:** 10.1088/1674-1056/20/8/085201

1. Introduction

The attosecond pulse is a powerful tool for the study of ultrafast processes in atoms, molecules, and solids. High-order harmonic generation (HHG) from relativistic laser pulses interacting with overdense plasma has been identified as a promising way to generate short wavelength radiation and attosecond pulses.[1−9] With the advent of the laser technique, the laser-focused intensity reaches relativistic range $I \geq 10^{18}$ W/cm^2. Recently, extreme light infrastructure (ELI)[10] has gone beyond the relativistic regime and forayed into the ultra-relativistic domain $I > 10^{24}$ W/cm^2. The laser normalized vector potential $a_0 = eA/(mc^2) = \left[I\left(\mathrm{W}\cdot\mathrm{cm}^{-2}\right)\lambda^2\left(\mu\mathrm{m}^2\right)/\left(1.37\times10^{18}\right)\right]^{1/2}$, where e and m are respectively the electron charge and mass, A is the amplitude of the laser electric field, c is the vacuum light velocity, and λ is the laser wavelength. The relativistic threshold is found for $a_0 \sim 1$. The laser pulse in the relativistic regime is usually over several cycles long, so the generated attosecond pulses from the reflected radiation are a pulse train.

The application of the attosecond pulse like molecular imaging[11,12] and quantum control[13] usually calls for a single attosecond pulse. The way to obtain a single subfemtosecond pulse via control atomic response by time-dependent laser polarization in the intense-field region was proposed by Ivanov *et al.*[14] in 1995. The time-dependent laser polarization method is also one of the schemes that have been proposed to obtain a single pulse from the interaction of a relativistic laser with overdense plasma.

The theory of high-order harmonic generation in relativistic laser interaction with overdense plasma was presented systematically by Baeva *et al.*[15] in 2006. They developed the theory of relativistic spikes and showed that the spectrum of the high-order harmonics is universal with slow power-law decay. In the same year, they[16] showed that a single attosecond X-ray burst from the managed time-dependent polarization laser pulse incident on a plasma surface can be obtained.

The first experimental results obtained using two laser beams for high-order harmonic generation from solids were presented by Tarasevitch *et al.*[17] in 2009. They discussed the advantages of using a two-beam (driver-probe) scheme to generate a high-order harmonic from solids and found that the two-pulse technique allows the additional control of the parameters essential for the generation of attosecond pulses. According to the synthesis of recent experimental results, Thaury and Quéré[18] improved the mechanism that indeed dominates the high-order harmonic generation

*Project supported by the Natural Science Foundation of Shandong Province of China (Grant No. ZR2009AQ009) and the National Basic Research Program of China (Grant No. 2011CB808100).

†Corresponding author. E-mail: qjzhang@sdnu.edu.cn

© 2011 Chinese Physical Society and IOP Publishing Ltd

and showed it is a plasma mirror.

The polarization of incident laser pulses can be managed by two perpendicularly polarized pulses with different amplitudes, frequencies, and phases. The pulse with a larger amplitude is the driving pulse and the other is the controlling pulse.

In this paper, we discuss the influence of the controlling pulse parameter on attosecond pulse generation. The results show that the attosecond pulse train generated can be controlled well by the controlling pulse parameter. The number and interval of the generated attosecond pulses are dominated by the frequency of the controlling pulse. The generation moment of the attosecond pulse varies accordingly by the phase difference between the controlling and driving pulses, and the amplitude of the controlling pulse affects the intensity of the attosecond pulse.

2. Theoretical model of the time-dependent polarization method

Here, we consider attosecond pulse generation from the interaction of a short ultrarelativistic laser pulse with overdense plasma. Because the mass of ions is larger, the response of the ions to the laser is slow. Therefore we suppose that the plasma ions are immobile and consider the electron motion only. The electrons in the plasma surface oscillate under the actions of the laser-light pressure and the restoring electrostatic force from the ions, so the electron gains a normal momentum component. And since the plasma is overdense, the incident laser pulse cannot penetrate it. As a consequence, there is an electric current flowing along the plasma surface, so the electron momentum in the plasma surface has both a normal component $P_{\rm n}$ and a tangential component P_τ, related by

$$P = \gamma m_{\rm e} v = \sqrt{P_{\rm n}^2 + P_\tau^2}, \tag{1}$$

where $\gamma = 1/\sqrt{1 - v^2/c^2}$ is the relativistic factor of the plasma surface.

So the velocity of the electrons in the plasma skin layer is

$$v_{\rm s} = c\sqrt{\frac{P_{\rm n}^2 + P_\tau^2}{m_{\rm e}^2 c^2 + P_{\rm n}^2 + P_\tau^2}}. \tag{2}$$

When the electrons move towards the laser pulse and the tangential electron momentum vanishes, $v_{\rm s}$ reaches its maximum c, and γ has a sharp peak, and high-order harmonics of the incident laser can be seen in the reflected radiation. After the proper filtering of the reflected radiation, we can obtain a train of attosecond pulses. In the one-dimensional (1D) geometry, the tangential component of the electron momentum is conserved: $P_\tau = eA_z/c$, where A_z is the tangential component of the vector potential $\boldsymbol{A}$. If the vector potential vanishes at several moments, several attosecond pulses in the reflected radiation are observed. For an elliptic polarization it never turns zero, while for a linear polarization it equals zero twice per laser period. So we generally obtain a train of attosecond pulses during the laser periods. For a laser pulse with time-dependent polarization, the number of the vector potential equals zero, dominated by the parameter of the controlling pulse. To obtain a single attosecond pulse, we can choose the proper parameter of the controlling pulse to ensure that the vector potential turns zero exactly once during the whole laser period.

Our analytical calculation and 1D particle-in-cell (PIC) simulations suggest that the parameter of the controlling pulse is sufficient to manage attosecond pulse generation. This means that the different attosecond pulses can be selected one by one or in groups out of the original pulse train by adjusting the amplitude, the frequency and the phase shift of the controlling pulse.

3. Analytical calculation of attosecond pulses with the time-dependent polarization method

The laser pulses with a Gaussian envelope $\boldsymbol{a}_1(t) = a_1 \exp\left(-t^2/4T^2\right) \sin\left(\omega_0 t\right) \hat{x}$ and $\boldsymbol{a}_2(t) = a_2 \exp\left(-t^2/4T^2\right) \sin\left(\omega_{\rm c} t + \Delta\phi\right) \hat{y}$ are used, where a_1, a_2, ω_0, and $\omega_{\rm c}$ are the amplitudes and the frequencies of the driving pulse (p polarization) and the controlling pulse (s polarization), respectively. And the frequencies of the two laser pulses are both normalized to ω_0, named the normalized frequency $\omega_0 = 1$. $T = 2\pi/\omega_0$ is the oscillation period of driving laser, and $\Delta\phi$ is the phase difference between the driving and controlling pulses. The superposition field with time-dependent polarization then comes into being while the two pulses are incident on the overdense plasma synchronously. The number of $\omega_0 t$ meeting

$\sin(\omega_0 t) = \sin(\omega_c t + \Delta\phi) = 0$ is the number of $A_z = 0$ within the pulse duration.

When the frequencies of the laser pulses are $\omega_0 = 1$ and $\omega_c = 1.25$, the phase difference $\Delta\phi$ varies from $\pi/16$ to π, and we find that A_z vanishes only when $\Delta\phi$ equals $\pi/4$, $\pi/2$, $3\pi/4$ or π separately. The moment of attosecond pulse generation is shown in Table 1. In the pulse duration, A_z turns into zero four times, and the interval is 4π, which means that there appear 4 attosecond pulses in the attosecond pulse train generated, as shown in Table 1. When the phase difference varies, the moment of attosecond pulse generation changes, but the number and interval of the attosecond pulse generation in the attosecond pulse train are unchanged. By increasing the phase difference until 2π, it turns out that the case of $\Delta\phi$ has the same result as that in the case of $\pi + \Delta\phi$.

Table 1. Dependence of attosecond pulse generation on the phase difference for $\omega_0 = 1$ and $\omega_c = 1.25$.

$\Delta\phi$	$\omega_0 t_1$	$\omega_0 t_2$	$\omega_0 t_3$	$\omega_0 t_4$
$\pi/2$	-6π	-2π	2π	6π
$3\pi/4$	-7π	-3π	π	5π
π	-8π	-4π	0	4π

When the frequency of the controlling pulse varies, the moment and the number of attosecond pulses generated change accordingly, as shown in Table 2. When $\omega_c = 1.5$ and $\Delta\phi = \pi/2$, A_z turns to zero eight times, the interval is 2π, which means that there are 8 attosecond pulses generated in the pulse duration (see Table 2).

Table 2. Dependences of moment $\omega_0 t_i$ and interval $\omega_0 \Delta t$ for attosecond pulse generation on ω_c and phase deference $\Delta\phi$.

ω_c	$\Delta\phi$	$\omega_0 \Delta t$	$\omega_0 t_i$ $(i = 1, 2, 3, \ldots)$
1.5	$\pi/2$	2π	$-7\pi, -5\pi, -3\pi, -\pi, \pi, 3\pi, 5\pi, 7\pi$
1.25	$\pi/4$	4π	$-5\pi, -\pi, 3\pi, 7\pi$
1.2	$\pi/5$	5π	$-6\pi, -\pi, 4\pi$
1.125	$\pi/8$	8π	$-\pi, 7\pi$

The vector potential of the laser pulse is represented as a function of time in Fig. 1, with the amplitude of driver pulse $a_0 = 30$ and frequency $\omega_0 = 1$. In Fig. 1(a), the amplitude of controlling pulse is $a_c = 15$, frequency $\omega_c = 1.5$, and phase difference $\Delta\phi = \pi/2$. As shown in Table 2, A_z turns to zero when $\omega_0 t = -7\pi, -5\pi, -3\pi, -\pi, \pi, 3\pi, 5\pi, 7\pi$, the corresponding points A–H are presented in Fig. 1(a). While the controlling pulse with amplitude $a_c = 15$, frequency $\omega_c = 1.25$ and phase shift $\Delta\phi = \pi/4$ is presented in Fig. 1(b). As shown in Table 2, A_z equals zero at $\omega_0 t = -5\pi, -\pi, 3\pi, 7\pi$, corresponding to the points A, B, C, and D in Fig. 1(b).

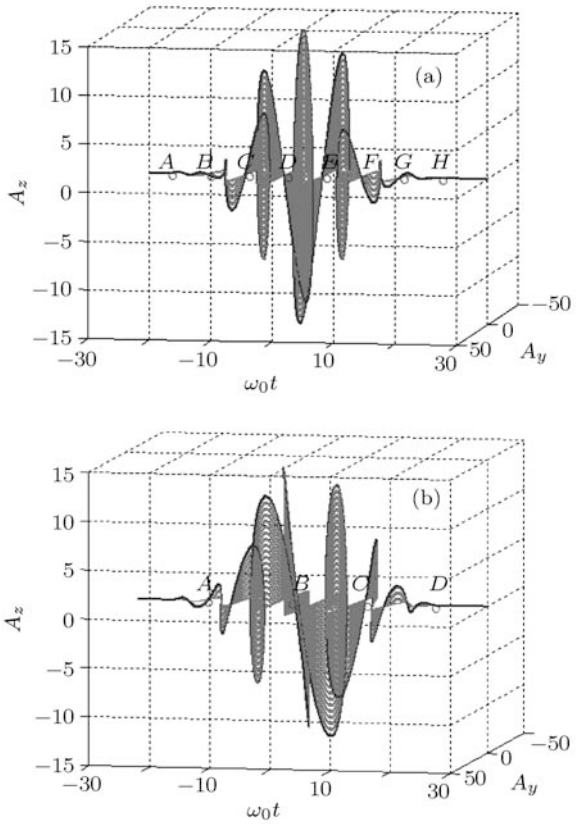


Fig. 1. Vector potential of the incident laser pulse for the driving pulse with $a_0 = 30$ and $\omega_0 = 1$. Panel (a) shows the controlling pulse with amplitude $a_c = 15$, frequency $\omega_c = 1.5$ and phase shift $\Delta\phi = \pi/2$; panel (b) exhibits the controlling pulse with amplitude $a_c = 15$, frequency $\omega_c = 1.25$ and phase shift $\Delta\phi = \pi/4$.

4. Results of PIC simulations

In this section, we show the corresponding results of PIC simulations. Here a dense plasma slab is exploited with $n_e/n_c = 90$, where n_e is the plasma electron density, and $n_c = \omega_0^2 m/4\pi e^2$ is the critical density for the laser pulse with the frequency ω_0. The plasma slab is positioned between $x_L = 4\lambda$ and $x_R = 9\lambda$. Take 5000 cells/λ and 100 particles per cell, where $\lambda = 2\pi/\omega_0 = 800$ nm is the driving laser pulse wavelength. At every time step, the incident and reflected fields are recorded at $x = 3.5\lambda$ (the position of the "external observer"). For the same parameters of driving and controlling pulses that were presented in Section 3, the moment of the central part of the incident pulse recorded is $\omega_0 t/2\pi = 15.5$. We use a high-pass filter to select harmonics above $n = 60$ for the reflected radiation. A train of attosecond pulses can be obtained by anti-Fourier transform of the filtered spectrum.

The temporal profile of the attosecond pulse train generated is shown in Fig. 2 with the amplitude of controlling pulse $a_c = 15$, frequency $\omega_c = 1.5$, and

phase shift $\Delta\phi = \pi/2$, where a_r represents the intensity of the reflected signal. There are 5 attosecond pulses in Fig. 2, corresponding to the points B–F in Fig. 1(a). The interval of the adjacent attosecod pulses is $\omega_0 t = 2\pi$, consistent with the corresponding analytical results. The strongest attosecond pulse is generated at the moment prior to the peak of the incident pulse for $\omega_0 t/2\pi = 0.5$, corresponding to the case of $\omega_0 t_i = \pi$ in analytical results. These results show that the simulation results are in good agreement with the analytical results. Meanwhile, the attosecond pulses that correspond to the points A, G, H in Fig. 1(a) are not observed. This is because these points are too far from the peak of the incident pulse to generate an observable attosecond pulse with enough intensity.

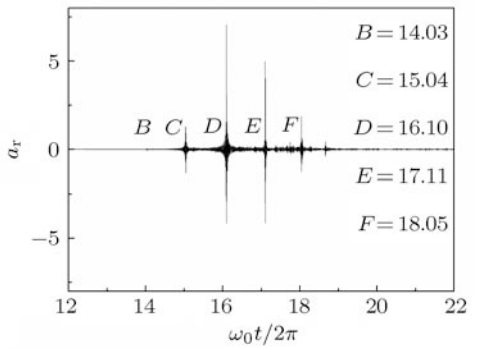


Fig. 2. Attosecond pulse train after spectral filtering for the controlling pulse with amplitude $a_c = 15$, frequency $\omega_c = 1.5$, and phase shift $\Delta\phi = \pi/2$.

When the amplitude of the controlling pulse $a_c = 10$, frequency $\omega_c = 1.2$, and the phase difference $\Delta\phi = \pi/5$, the temporal profile of the attosecond pulses is shown in Fig. 3. There are 3 attosecond pulses in Fig. 3. The interval is $\omega_0 t/2\pi = 2.5$, corresponding to $\omega_0 t_i = 5\pi$ in the analytical results. The strongest attosecond pulse is also generated at the moment prior to the peak of the incident pulse for $\omega_0 t/2\pi = 0.5$, corresponding to that in the case of $\omega_0 t_i = \pi$ in the analytical results. These attosecond pulses fit in well with the analytical results. For the same reason, the points A and C are too far from the peak of the incident pulse to generate an observable attosecond pulse with enough intensity, so it looks as if we select a single attosecond pulse out of the train.

The influence of the controlling pulse phase shift on the attosecond pulse is studied as follows. The temporal profile of the attosecond pulses is shown in Fig. 4 for the controlling pulse with amplitude $a_c = 15$, frequency $\omega_c = 1.5$, and the phase shift $\Delta\phi = \pi$. When the phase shift changes, the moment of attosecond pulse generation changes (see Figs. 2 and 4), but there are 5 attosecond pulses in the pulse train and the interval of the attosecond pulse is still $\omega_0 t/2\pi = 1$. This is consistent with the analytical results.

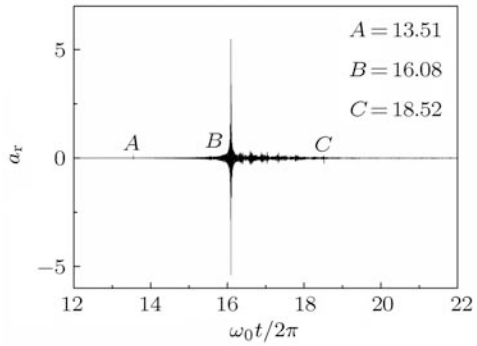


Fig. 3. Attosecond pulse train after spectral filtering for the controlling pulse with amplitude $a_c = 10$, frequency $\omega_c = 1.2$, and phase shift $\Delta\phi = \pi/5$.

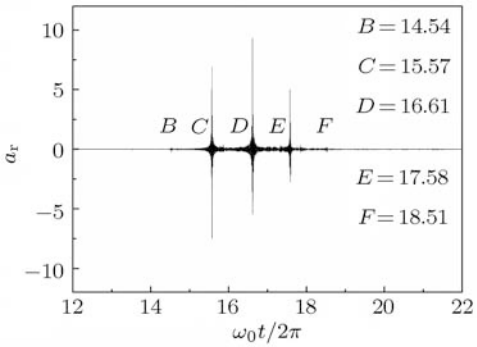


Fig. 4. Attosecond pulse train after spectral filtering for the controlling pulse with amplitude $a_c = 15$, frequency $\omega_c = 1.5$, and phase shift $\Delta\phi = \pi$.

Finally, the influence of the controlling pulse amplitude on attosecond pulses is discussed. Figure 5 shows the temporal profile of the attosecond pulses for the case of the controlling pulse with amplitude $a_c = 15$, frequency $\omega_c = 1.2$, and the phase shift $\Delta\phi = \pi/5$. With the same frequency and phase shift, but different amplitudes as shown in Figs 3 and 5,

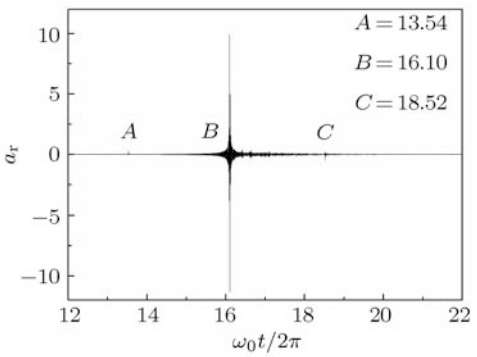


Fig. 5. Attosecond pulse train after spectral filtering for the controlling pulse with amplitude $a_c = 15$, frequency $\omega_c = 1.2$, and phase shift $\Delta\phi = \pi/5$.

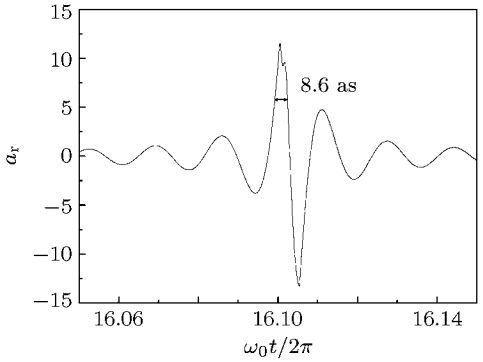


Fig. 6. Maximum attosecond pulse after spectral filtering for the controlling pulse with amplitude $a_c = 15$, frequency $\omega_c = 1.2$, and phase shift $\Delta\phi = \pi/5$.

the moment, the number and the interval of attosecond pulse generation remain unvaried; only the intensity of the attosecond pulse changes. The maximum attosecond pulse in Fig. 5 is shown solely in Fig. 6. We can see that this "single" pulse has a duration $\tau \approx 8.6$ as and intensity $I \approx 3.08 \times 10^{20}$ W/cm^2. The intensity ratio of the attosecond pulse to the driving pulse is 40%. This means that choosing an appropriate amplitude, we can gain an ideal single attosecond pulse. With regard to the dependences of attosecond pulse generation on the driving pulse amplitude and the plasma density, these were shown in our previous work.[19]

5. Conclusion

In this work, the influence of time-dependent polarization on attosecond pulse generation from the overdense plasma surface driven by a laser pulse is discussed analytically and numerically. The interval and the number of attosecond pulses in the attosecond pulse train can be changed by the frequency of the controlling pulse, and the moment of attosecond pulse generation is controlled by the phase difference between two incident laser pulses. These results in PIC simulations are consistent with those obtained from analytical methods. And because the intensity of the attosecond pulse is affected by the amplitude of the controlling pulse, we can "select" a single attosecond pulse with high intensity by choosing an appropriate parameter of the controlling pulse, so the time-dependent polarization method will be a possible way to realize applications of the attosecond pulse.

References

[1] Gordienko S, Pukhov A, Shorokhov O and Baeva T 2004 *Phys. Rev. Lett.* **93** 115002

[2] Cai H B, Yu W, Zhu S P and Zhou C T 2007 *Phys. Rev.* E **76** 036403

[3] Hong W Y, Lan P F, Lu P X and Yang Z Y 2008 *Acta Phys. Sin.* **57** 5853 (in Chinese)

[4] Watts I, Zepf M, Clark E L, Tatarakis M, Krushelnick K and Dangor A E 2002 *Phys. Rev. Lett.* **88** 155001

[5] Cao W, Lan P F and Lu P X 2007 *Acta Phys. Sin.* **56** 1608 (in Chinese)

[6] Huang Z Q and Wang H Y 2005 *Chin. Phys.* **14** 2560

[7] Eidmann K, Kawachi T, Marcinkevičius A, Bartlome R, Tsakiris G D and Witte K 2005 *Phys. Rev.* E **72** 036413

[8] Lichters R, Meyer-ter-Vehn J and Pukhov A 1996 *Phys. Plasmas* **3** 3425

[9] Gordienko S, Pukhov A, Shorokhov O and Baeva T 2005 *Phys. Rev. Lett.* **94** 103903

[10] Mourou G A, Labaune C L, Dunne M, Naumova N and Tikhonchuk V T 2007 *Plasma Phys. Control Fusion* **49** B667

[11] Itatani J, Levesque J, Zeidler D, Niikura H, Pèpin H, Kieffer J C, Corkum P B and Villeneuve D M 2004 *Nature* (London) **432** 867

[12] Lein M, Hay N, Velotta R, Marangos J P and Knight P L 2002 *Phys. Rev.* A **66** 023805

[13] Rabitz H, de Vivie-Riedle R, Motzkus M and Kompa K 2000 *Science* **288** 824

[14] Ivanov M, Corkum P B, Zuo T and Bandrauk A 1995 *Phys. Rev. Lett.* **74** 2933

[15] Baeva T, Gordienko S and Pukhov A 2006 *Phys. Rev.* E **74** 046404

[16] Baeva T, Gordienko S and Pukhov A 2006 *Phys. Rev.* E **74** 065401

[17] Tarasevitch A P, Kohn R and von der Linde D 2009 *J. Phys.* B: *At. Mol. Opt. Phys.* **42** 134006

[18] Thaury C and Quéré F 2010 *J. Phys.* B: *At. Mol. Opt. Phys.* **43** 213001

[19] Luo M H, Zhang Q J and Yan C Y 2010 *Acta Phys. Sin.* **59** 8559 (in Chinese)